Eight-Degrees-of-Freedom Remote Actuation of Small Magnetic Mechanisms

Sajad Salmanipour and Eric Diller

***Abstract*— Magnetically-driven micrometer to millimeter-scale robotic devices have recently shown great capabilities for remote applications in medical procedures, in microfluidic tools and in microfactories. Significant effort recently has been on the creation of mobile or stationary devices with multiple independently-controllable degrees of freedom (DOF) for multi-agent or complex mechanism motions. In most applications of magnetic microrobots, however, the relatively large distance from the field generation source and the microscale devices results in controlling magnetic field signals which are applied uniformly over all agents. While some progress has been made in this area allowing up to six independent DOF to be individually commanded, there has been no rigorous effort in determining the maximum achievable number of DOF for systems with uniform magnetic field input. In this work, we show that this maximum is eight and we introduce the theoretical basis for this conclusion, relying on the number of independent usable components in a magnetic field at a point. In order to verify the claim experimentally, we develop a simple demonstration mechanism with 8 DOF designed specifically to show independent actuation. Using this mechanism with 500 μm magnetic elements, we demonstrate eight independent motions of 0.6 mm with 8.6 % coupling using an eight coil system. These results will enable the creation of richer outputs in future microrobotic devices.**

I. INTRODUCTION

Progress in the wireless control of microrobots has demonstrated the potential of the field in applications such as microfluidics, drug delivery and minimal invasive surgery, where the challenge is to remotely control and actuate microscale devices without physical access to the workspace. Recently, there has been a wide variety of innovative and successful methods developed for remote actuation and control in microscale, with actuation based on magnetism [1], [2], electrostatic forces [3], chemical reactions [4], thermal activation [5], optical [6] and even bacteria motility-based [7] techniques.

At small size scales, one particular challenge is in providing power for remote agents in order to generate relatively large forces and torques. Another major challenge is to individually address different motions of remote agents and control them independently for team or multi-degree of freedom (DOF) motions within one workspace. Considering both challenges, magnetic-based actuation is commonly used, where in addition to its ability to generate relatively large forces and torques, magnetic actuation does not require on-board selection modules to achieve multiple controllable DOFs. Wireless magnetic actuation would allow for multi DOF systems that is not possible with other techniques without a compromise in their size or actuation forces [8], [9].

Magnetic-based approaches featuring multi-agent or multi-DOF control can be categorized by their control with assumptions of uniform or non-uniform magnetic fields over the operating workspace. Uniform fields are assumed in applications where the displacements of remote agents are negligible compared to distance of magnetic sources from the workspace [2] and thus the external magnetic field can be considered uniform over the workspace. This assumption is usually considered valid for most medical applications where the field sources must be located outside the body. On the other hand, when agents displacements are large compared with the distance to the field source, it should be assumed that the external magnetic field varies over the workspace [10], a fact which could be used for independent control [11]. In this paper we focus on the former case where a uniform magnetic field assumption is made; in other words, we analyze magnetic field components at a single point in workspace. This makes it a more comprehensive study, where analyzing magnetic fields at a single point, determines capabilities of both, uniform and non-uniform fields.

One approach to achieve multiple DOFs in the uniform field case is through time-encoded signals. Becker et al., for example, suggest a mechanical decoding system for modulated magnetic control signals [12]. However, this method requires relatively large agents in an MRI which is not feasible in microscale and can not be generalized to other microrobotic systems. In this work, on the other hand, we consider steady magnetic actuation; in other words, where magnetic fields are in steady state and actuation forces and torques can be seen as linearly dependent on field and field gradient inputs. Thus the results of this study can be applied to more complex actuation types including both steady and time-dependent signals.

In a steady uniform magnetic field, actuation power is transmitted to remote magnetic devices by the application of magnetic torque and magnetic force. The magnetic field, denoted by the vector $[B_x \ B_y \ B_z]^\top$ induces a rigid-body torque, while the spatial gradient of the field generates a force. There has been significant effort in exploiting magnetic torque capabilities in order to actuate micro-robots, including helical-based [1], [13] or traveling-wave propulsion methods [14], [15]. However, torque-actuated mechanisms have at most three independent control inputs, one each for the

*This work is supported by the NSERC Discovery Grants Program.

S. Salmanipour and E. Diller are with the department of Mechanical and Industrial Engineering, University of Toronto, 5 Kings College Road, Toronto, M5S 3G8, Canada. ediller@mie.utoronto.ca

independent components of the magnetic field vector at a point (B_x, B_y, B_z). As a result, the number of independent DOFs can not exceed three for torque-only actuation. Therefore, in order to achieve more than 3 DOFs, the gradient of magnetic field should also be used. By developing systems capable of controlling both magnetic field and its gradient to apply force in addition to torques, current designs in the literature have achieved 5 DOF [2], [16] (3 DOF positioning and 2 DOF orientation control of a rigid body microdevice) and up to 6 DOF magnetic systems [17], [18]. (3 DOF positioning and 3 DOF orientation control). While it has been noted that the magnetic field and its gradient contain eight independent components at any point in space (which has served as justification for the use of a minimum of eight actuating magnetic coils in many of these systems [19]), microsystems with only up to 6 DOF have been developed in previous designs. A single rigid body has only 6 DOF, however, more complex systems such as multi-agent systems or those containing jointed or flexible mechanisms [20] can have many more free DOF which would be useful to control.

In this work, we first investigate the magnetic field and its gradient to determine the theoretical maximum number of independent controllable inputs for a generic magnetic system operating at a point in space under the influence of a uniform field input. Based on the available independent parameters of the field and its gradient at a point, we show that this number of independent inputs is eight. To demonstrate this independent actuation, we design a magnetically-driven system in a way that those eight independently controllable inputs result in eight independently controllable outputs. The proposed 8 DOF magnetic mechanism consists of two parts, a magnetic field generation system and remote mm-scale magnetic agents (which could be generalized to any small-scale magnetic remote devices). Since a rigid body cannot have more than 6 DOF, a system with eight outputs requires at least two bodies. For a simple demonstration, we use seven agents (possessing total of 8 DOF), requiring only one camera to measure all of the eight outputs. We show calibration and validation of the experimental system, and demonstrate 8 DOF actuation, where all of its 8 DOFs can be individually addressed and actuated with a maximum coupling of 8.6%. Thus, for the first time, we investigate the capability of steady uniform magnetic fields to achieve a wireless mechanism with maximum number of DOFs which is eight. This work serves as a proof of concept which will enable more dexterous actuation of future wireless magnetic mechanisms with maximum dexterity.

II. MAGNETIC ACTUATION

In this section, magnetic actuation principles are introduced, with force and torque equations written in matrix form as the basis for discussing our scheme for full-DOF actuation. These equations are utilized to investigate the theoretical maximum number of DOFs, and we limit discussion to systems utilizing steady uniform magnetic fields only.

A. Background on Magnetic Field Actuation

Maxwell's equations describe a magnetic field in a free-current workspace as:

$$\nabla \cdot \vec{B} = 0 \tag{1}$$

$$\nabla \times \vec{B} = 0 \tag{2}$$

where $\vec{B}_{3\times1}$ is the magnetic field vector. This magnetic field results in a force $\vec{F}_{3\times1}$ and a torque vector $\vec{\tau}_{3\times1}$ acting on the magnetic agent (the remote micro-device), calculated as:

$$\vec{F} = (\vec{m} \cdot \nabla)\vec{B} \tag{3}$$

$$\vec{\tau} = \vec{m} \times \vec{B} \tag{4}$$

where $\vec{m} = [m_x\ m_y\ m_z]^\top$ is the dipole moment of the magnetic agent. Using cross product identities, the torque equation (4) can be rewritten in matrix form as:

$$\vec{\tau} = \begin{bmatrix} \tau_x \\ \tau_y \\ \tau_z \end{bmatrix} = \begin{bmatrix} 0 & -m_z & m_y \\ m_z & 0 & -m_x \\ -m_y & m_x & 0 \end{bmatrix} \begin{bmatrix} B_x \\ B_y \\ B_z \end{bmatrix} \tag{5}$$

In order to also write the force equation (3) in a matrix form, Maxwell's equations are utilized. Equation (1) implies that gradient of the magnetic field vector has a zero trace and (2) constrains it to be symmetric. As a result, equation (3) can be rewritten as:

$$\vec{F} = \begin{bmatrix} \frac{\partial B_x}{\partial x} & \frac{\partial B_x}{\partial y} & \frac{\partial B_x}{\partial z} \\ \frac{\partial B_x}{\partial y} & \frac{\partial B_y}{\partial y} & \frac{\partial B_y}{\partial z} \\ \frac{\partial B_x}{\partial z} & \frac{\partial B_y}{\partial z} & -\left(\frac{\partial B_y}{\partial y} + \frac{\partial B_x}{\partial x}\right) \end{bmatrix} \begin{bmatrix} m_x \\ m_y \\ m_z \end{bmatrix} \tag{6}$$

As it can be seen from (6), the gradient matrix has five independent components [19]. By rearranging them into a 5×1 vector, equation (6) can be simplified to:

$$\vec{F} = \begin{bmatrix} f_x \\ f_y \\ f_z \end{bmatrix} = \begin{bmatrix} m_x & m_y & m_z & 0 & 0 \\ 0 & m_x & 0 & m_y & m_z \\ -m_z & 0 & m_x & -m_z & m_y \end{bmatrix} \begin{bmatrix} \frac{\partial B_x}{\partial x} \\ \frac{\partial B_x}{\partial y} \\ \frac{\partial B_x}{\partial z} \\ \frac{\partial B_y}{\partial y} \\ \frac{\partial B_y}{\partial z} \end{bmatrix} \tag{7}$$

B. Multi-DOF Magnetic Actuation

Using equations (5) and (7), exerted force and torque on a magnetic device with magnetization vector $\vec{m} = \begin{bmatrix} m_x & m_y & m_z \end{bmatrix}^\top$, can be summarized in a matrix form as:

$$\begin{bmatrix} f_x \\ f_y \\ f_z \\ \tau_x \\ \tau_y \\ \tau_z \end{bmatrix} = \begin{bmatrix} m_x & m_y & m_z & 0 & 0 & 0 & 0 & 0 \\ 0 & m_x & 0 & m_y & m_z & 0 & 0 & 0 \\ -m_z & 0 & m_x & -m_z & m_y & 0 & 0 & 0 \\ 0 & 0 & 0 & 0 & 0 & 0 & -m_z & m_y \\ 0 & 0 & 0 & 0 & 0 & m_z & 0 & -m_x \\ 0 & 0 & 0 & 0 & 0 & -m_y & m_x & 0 \end{bmatrix} \vec{U} \tag{8}$$

$$\vec{U} = \begin{bmatrix} \frac{\partial B_x}{\partial x} & \frac{\partial B_x}{\partial y} & \frac{\partial B_x}{\partial z} & \frac{\partial B_y}{\partial y} & \frac{\partial B_y}{\partial z} & B_x & B_y & B_z \end{bmatrix}^\top$$

A combination of forces and torques can be used to actuate remote magnetic agents. System output depends on this

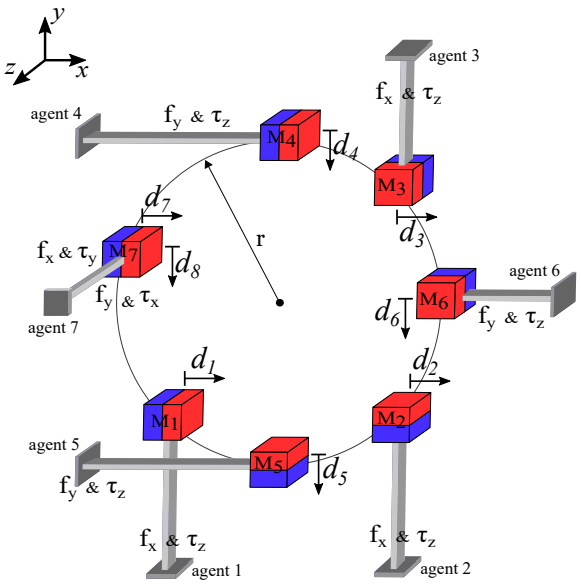

Fig. 1: 8 DOF magnetic mechanism used to demonstrate independent actuation. Remote magnetic agents are cubic permanent magnets, physically constrained to experience deflections along one (agents 1-6) or two axes (agent 7). Considering relatively small deflections, orientation of the net magnetization vector for each magnet is assumed to be fixed.

combination, whereas system input is always the same and we choose it be an 8×1 vector, named $\vec{U}$.

In order to investigate what is the maximum number of independent outputs in a local magnetic field, the input/output vectors must be studied. Based on equation (8), maximum number of independent outputs can not be greater than number of inputs which is eight. To validate the possibility of this maximum of eight, we designed a simple system with seven small magnets possessing eight free DOFs. As illustrated in Fig. 1, magnets are denoted by $\mathrm{M_i}$ $(i:1-7)$ and output displacements as d_i $(i:1-8)$. In this system, remote magnetic devices are simply cubic permanent magnets that are attached to flexible arms. As described in Table I, these flexible arms are physically constrained in a way that they can only experience deflections in one or two directions (each agent has 1 or 2 DOFs).

TABLE I: Specifications of the proposed 8 DOF magnetic mechanism.

Agent #	1	2	3	4	5	6	7
Number of DOFs	1	1	1	1	1	1	2
Output	d_1	d_2	d_3	d_4	d_5	d_6	d_7, d_8
Motion Axis	x	x	x	y	y	y	x,y
Actuation Force	f_x	f_x	f_x	f_y	f_y	f_y	f_x, f_y
Actuation Torque	τ_z	τ_z	τ_z	τ_z	τ_z	τ_z	τ_y, τ_x
Orientation $\frac{\vec{m}_i}{\|\vec{m}_i\|}$	$\begin{bmatrix}1\\0\\0\end{bmatrix}$	$\begin{bmatrix}0\\1\\0\end{bmatrix}$	$\begin{bmatrix}0\\0\\1\end{bmatrix}$	$\begin{bmatrix}1\\0\\0\end{bmatrix}$	$\begin{bmatrix}0\\1\\0\end{bmatrix}$	$\begin{bmatrix}0\\0\\1\end{bmatrix}$	$\begin{bmatrix}1\\0\\0\end{bmatrix}$

There are 8 DOFs in total where each one of them is actuated by a force element (f_x or f_y) and a torque element (τ_x or τ_y or τ_z). By choosing d_1-d_8 as outputs, system output vector $\vec{Y}$ is calculated as:

$$\vec{Y} = \begin{bmatrix} d_1 & d_2 & d_3 & d_4 & d_5 & d_6 & d_7 & d_8 \end{bmatrix}^\top \tag{9}$$
$$d_1 = +\alpha f_{1x} - \beta \tau_{1z} \quad d_2 = +\alpha f_{2x} - \beta \tau_{2z} \quad d_3 = +\alpha f_{3x} - \beta \tau_{3z}$$
$$d_4 = -\alpha f_{4y} - \beta \tau_{4z} \quad d_5 = -\alpha f_{5y} - \beta \tau_{5z} \quad d_6 = -\alpha f_{6y} - \beta \tau_{6z}$$
$$d_7 = +\alpha f_{7x} - \beta \tau_{7y} \quad d_8 = -\alpha f_{7y} - \beta \tau_{7x}$$

where α and β are constant scalars mapping from force and torque inputs to deflection outputs, respectively. Using (8), equation (9) can be written in matrix form as:

$$\vec{Y} = \begin{bmatrix} m_{1x} & m_{1y} & m_{1z} & 0 & 0 & m_{1y} & -m_{1x} & 0 \\ m_{2x} & m_{2y} & m_{2z} & 0 & 0 & m_{2y} & -m_{2x} & 0 \\ m_{3x} & m_{3y} & m_{3z} & 0 & 0 & m_{3y} & -m_{3x} & 0 \\ 0 & -m_{4x} & 0 & -m_{4y} & -m_{4z} & m_{4y} & -m_{4x} & 0 \\ 0 & -m_{5x} & 0 & -m_{5y} & -m_{5z} & m_{5y} & -m_{5x} & 0 \\ 0 & -m_{6x} & 0 & -m_{6y} & -m_{6z} & m_{6y} & -m_{6x} & 0 \\ m_{7x} & m_{7y} & m_{7z} & 0 & 0 & -m_{7z} & 0 & m_{7x} \\ 0 & -m_{7x} & 0 & -m_{7y} & -m_{7z} & 0 & m_{7z} & -m_{7y} \end{bmatrix} \boldsymbol{\lambda}\, \vec{U}$$
$$\vec{Y} = \mathbf{K}\, \boldsymbol{\lambda}\, \vec{U}$$
$$\vec{Y} = \mathbf{S}\, \vec{U} \tag{10}$$
$$\mathbf{S}_{8\times 8} = \mathbf{K}_{8\times 8}\ \boldsymbol{\lambda}_{8\times 8}$$
$$\boldsymbol{\lambda}_{8\times 8} = diag(\alpha,\alpha,\alpha,\alpha,\alpha,\beta,\beta,\beta)$$

Here, $\mathbf{S}$ represents the system matrix which maps from the input vector $\vec{U}$ to output $\vec{Y}$. In order to be able to have full control over all of the eight outputs, system matrix $\mathbf{S}$ must be full rank. As equation (10) shows, for a full rank matrix, magnetization vectors of agents which have the same motion axis (agents 1-3 and 4-6) must be linearly independent, and the magnetization vector for the last agent must have a non-zero component in $x-y$ plane. Therefore, we choose magnetization vectors for the agents as:

$$\vec{m}_1 = \vec{m}_4 = \begin{bmatrix}\gamma & 0 & 0\end{bmatrix}^\top \quad \vec{m}_2 = \vec{m}_5 = \begin{bmatrix}0 & \gamma & 0\end{bmatrix}^\top$$
$$\vec{m}_3 = \vec{m}_6 = \begin{bmatrix}0 & 0 & \gamma\end{bmatrix}^\top \quad \vec{m}_7 = \begin{bmatrix}\gamma & 0 & 0\end{bmatrix}^\top \tag{11}$$

where γ is a scalar representing the magnitude of magnetization vectors (same for all). By inserting (11) into (10), system matrix $\mathbf{S}$ is calculated as:

$$\mathbf{S} = \begin{bmatrix} \alpha\gamma & 0 & 0 & 0 & 0 & 0 & -\beta\gamma & 0 \\ 0 & \alpha\gamma & 0 & 0 & 0 & \beta\gamma & 0 & 0 \\ 0 & 0 & \alpha\gamma & 0 & 0 & 0 & 0 & 0 \\ 0 & -\alpha\gamma & 0 & 0 & 0 & 0 & -\beta\gamma & 0 \\ 0 & 0 & 0 & -\alpha\gamma & 0 & \beta\gamma & 0 & 0 \\ 0 & 0 & 0 & 0 & -\alpha\gamma & 0 & 0 & 0 \\ \alpha\gamma & 0 & 0 & 0 & 0 & 0 & 0 & \beta\gamma \\ 0 & -\alpha\gamma & 0 & 0 & 0 & 0 & 0 & 0 \end{bmatrix} \tag{12}$$

where its determinant is equal to:

$$|\mathbf{S}| = -\alpha^5\ \beta^3\ \gamma^8 \tag{13}$$

As it can be seen from (13), if α, β and γ are non-zero, system matrix is full rank and all of the outputs d_1-d_8

can be controlled independently through the input vector $\vec{U}$. It should also be noted that this system matrix represents a linearized model of the system with fixed magnetization vectors $\vec{m}_1 - \vec{m}_7$, which is only valid when deflections are small enough. This criteria can be expressed as:

$$\sin(\theta) \approx 0 \qquad \theta = d_i/l_i \tag{14}$$

where l_i is the ith arm's length. In order to meet this condition, we choose our desired output deflections to be 20 times smaller than arms' lengths.

III. Generating Magnetic Field and Gradient

Having a full rank system matrix guarantees that system outputs can be controlled independently if we have full control over system inputs. In other words, we need to be able to control all of the eight terms in the $\vec{U}$ vector. To do so, we need a magnetic field generation system capable of simultaneously generating three field terms (B_x, B_y, B_z), and five gradient terms $(\frac{\partial B_x}{\partial x}, \frac{\partial B_x}{\partial y}, \frac{\partial B_x}{\partial z}, \frac{\partial B_y}{\partial y}, \frac{\partial B_y}{\partial z})$. As a result, at least eight independent magnetic field sources are needed. These sources can either be electromagnetic coils, permanent magnets or a combination of both. In this work, we chose to have eight electromagnetic coils as our controllable input sources.

Using the Bio-Savart law, magnetic field vector $\vec{B}$ and its gradient matrix $\mathbf{G}$, for a coil pointing toward $\vec{z}$ direction at a distance of D on its axis, can be calculated as:

$$\vec{B} = \rho \begin{bmatrix} 0 & 0 & 1 \end{bmatrix}^\top \qquad \rho = \frac{\mu_0 N i a^2}{2(a^2+D^2)^{1.5}} \tag{15}$$

$$\mathbf{G} = \begin{bmatrix} \frac{\partial B_x}{\partial x} & \frac{\partial B_x}{\partial y} & \frac{\partial B_x}{\partial z} \\ \frac{\partial B_x}{\partial y} & \frac{\partial B_y}{\partial y} & \frac{\partial B_y}{\partial z} \\ \frac{\partial B_x}{\partial z} & \frac{\partial B_y}{\partial z} & -(\frac{\partial B_y}{\partial y} + \frac{\partial B_x}{\partial x}) \end{bmatrix} = \sigma \begin{bmatrix} 1 & 0 & 0 \\ 0 & 1 & 0 \\ 0 & 0 & -2 \end{bmatrix} \tag{16}$$

$$\sigma = \frac{3\mu_0 N i a^2 D}{4(a^2+D^2)^{2.5}} \qquad \mu_0 = 4\pi \times 10^{-7} \text{T.m.A}^{-1}$$

where a is the coil radius, i is the current, N represents number of turns and μ_0 is the permeability of free space. Here we assumed the coil is pointing toward $\vec{z}$ axis, but using a rotation matrix $\mathbf{R}$, these calculations can be generalized for a coil with a desired axis $\vec{n}$, as:

$$\vec{B} = \mathbf{R} \begin{bmatrix} 0 & 0 & \rho \end{bmatrix}^\top \tag{17}$$

$$\mathbf{G} = \mathbf{R} \begin{bmatrix} \sigma & 0 & 0 \\ 0 & \sigma & 0 \\ 0 & 0 & -2\sigma \end{bmatrix} \mathbf{R}^\top \tag{18}$$

$$\vec{n} = \mathbf{R} \begin{bmatrix} 0 & 0 & 1 \end{bmatrix}^\top$$

Having eight coils positioned around workspace with different orientations, magnetic field and gradient terms can be calculated as:

$$\vec{U} = \mathbf{L}_{8\times 8}\, \vec{I}_{8\times 1} \tag{19}$$

$$\vec{U} = \begin{bmatrix} \frac{\partial B_x}{\partial x} & \frac{\partial B_x}{\partial y} & \frac{\partial B_x}{\partial z} & \frac{\partial B_y}{\partial y} & \frac{\partial B_y}{\partial z} & B_x & B_y & B_z \end{bmatrix}^\top$$

where $\mathbf{L}$ is the system matrix mapping from eight coil currents to the eight field and gradient terms. By utilizing

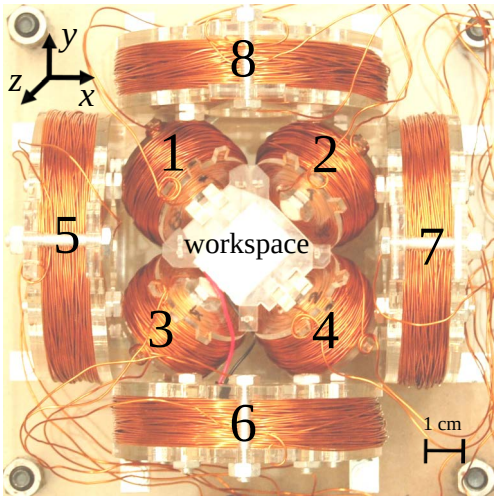

Fig. 2: Magnetic field generation prototype, consisting of four inner coils $(1-4)$ and four outer coils $(5-8)$. The system is capable of independently generating three magnetic field components as large as 15 mT, and five gradient components as large as 0.55 T/m.

equations (17) and (18) for each coil individually, columns of $\mathbf{L}$ matrix are calculated; where ith column maps from ith coil current $\vec{I}_i$ to $\vec{U}$.

The system is able to generate all eight field and gradient terms independently, if and only if $\mathbf{L}$ is full rank. In order to optimize coil configurations, MATLAB *fmincon* function (interior-point algorithm) was utilized. The parameters to be optimized were coils axes, their radius and their distance to workspace. Constraints were power limitations (maximum current of 15 A for each coil), workspace size (a circle with minimum radius of 3 cm, maximum of 4 cm) and $\mathbf{L}$ matrix rank (must be eight). The following cost function was also defined to maximize generated field and gradient components:

$$f = (\eta_1\ \vec{B}^\top \vec{B} + \eta_2\ \vec{g}^\top \vec{g})^{-1} \tag{20}$$

$$\vec{B} = \begin{bmatrix} B_x & B_y & B_z \end{bmatrix}^\top \qquad \vec{g} = \begin{bmatrix} \frac{\partial B_x}{\partial x} & \frac{\partial B_x}{\partial y} & \frac{\partial B_x}{\partial z} & \frac{\partial B_y}{\partial y} & \frac{\partial B_y}{\partial z} \end{bmatrix}^\top$$

where η_1 and η_2 are positive constant scalars.

The optimized solution has four outer coils with their centers in $x-y$ plane and four inner coils positioned below $x-y$ plane (30 degrees tilted). Figure 2, shows the final developed coil system and coils specifications can be found in Table II.

In order to calibrate the coil system, a test current of 10 A was sent to each coil separately and resulted data (Table III) were used to calculate the $\mathbf{L}$ matrix (equation (19)). Calculated matrix is full rank and considering our 15 A current limit, the system can reliably generate three magnetic field components as large as 15 mT, and five gradient components as large as 0.55 T/m.

TABLE II: Coils specifications; including radius a, distance to workspace center D, number of wire turns N, wire gauges and coils axes $\vec{n}$.

	a (cm)	D (cm)	N	Gauge	Coils axes ($\vec{n}$)
Coil 1	2.5	3.3	450	20	$[+0.6 \quad -0.6 \quad +0.5]^\top$
Coil 2	2.5	3.3	450	20	$[-0.6 \quad -0.6 \quad +0.5]^\top$
Coil 3	2.5	3.3	450	20	$[+0.6 \quad +0.6 \quad +0.5]^\top$
Coil 4	2.5	3.3	450	20	$[-0.6 \quad +0.6 \quad +0.5]^\top$
Coil 5	5.6	5.7	600	20	$[+1.0 \quad 0.0 \quad 0.0]^\top$
Coil 6	5.6	5.7	600	20	$[0.0 \quad +1.0 \quad 0.0]^\top$
Coil 7	5.6	5.7	600	20	$[-1.0 \quad 0.0 \quad 0.0]^\top$
Coil 8	5.6	5.7	600	20	$[0.0 \quad -1.0 \quad 0.0]^\top$

TABLE III: Coils characterization data; sending 10 A to each coil individually. Field components are measured using 3-axis gauss-meter (460, Lake Shore Cryotronics), and gradient components are estimated based on dipole model and measured field data.

	B_x(mT)	B_y(mT)	B_z(mT)	$\frac{\partial B_x}{\partial x}$ (T/m)	$\frac{\partial B_x}{\partial y}$ (T/m)	$\frac{\partial B_x}{\partial z}$ (T/m)	$\frac{\partial B_y}{\partial y}$ (T/m)	$\frac{\partial B_y}{\partial z}$ (T/m)
Coil 1	5.7	-5.8	4.5	-0.04	0.31	-0.24	-0.04	0.24
Coil 2	-4.1	-4.4	3.5	0.00	-0.22	0.17	-0.04	0.19
Coil 3	4.7	5.3	4.2	0.00	-0.26	-0.21	-0.05	-0.23
Coil 4	-5.1	4.7	3.8	-0.05	0.26	0.21	-0.01	-0.19
Coil 5	11.6	-0.1	0.0	-0.35	0.01	0.00	0.17	0.00
Coil 6	-0.1	10.7	0.4	-0.16	-0.01	0.00	0.33	0.02
Coil 7	-10.5	-0.5	-0.8	-0.32	-0.02	-0.03	0.16	0.00
Coil 8	1.2	-12.5	0.6	-0.18	-0.05	0.00	0.38	-0.03

IV. Experimental Results

As shown in Fig. 3a, the proposed 8 DOF magnetic mechanism was built using seven pieces of Nitinol wire (2.5 cm length, 75 μm diameter) as flexible arms attached to seven cubic permanent magnets (NdFeB, 500 μm). One stationary camera (FO134TC, Foculus) provided $x-y$ position measurements (Fig. 3b), with a LED plate placed beneath the workspace as its light source.

The magnetic field generation system and the 8 DOF magnetic mechanism can be considered as two systems working in series. By combining equations (10) and (19), we will have:

$$\vec{Y} = \mathbf{S}\,\mathbf{L}\,\vec{I} = \mathbf{H}\,\vec{I} \qquad (21)$$
$$\mathbf{H}_{8\times8} = \mathbf{S}_{8\times8}\,\mathbf{L}_{8\times8}$$

where $\mathbf{H}$ is the overall system matrix mapping from coil currents $\vec{I}$ to system output $\vec{Y}$. In order to determine this matrix, $\mathbf{S}$ must be calculated first. To do so, eight different input sets were applied and agents deflections were measured. The information specifying input sets are listed in Table IV, and the resulted measured deflections can be found in Table V.

Calibration results (Table V) were utilized to calculate $\mathbf{S}$ and consequently $\mathbf{H}$ matrix. The calculated $\mathbf{H}$ matrix is full rank, and considering the 15 A current limit for our coils, the system was able to actuate each one of the eight outputs with a maximum deflection of 800 μm.

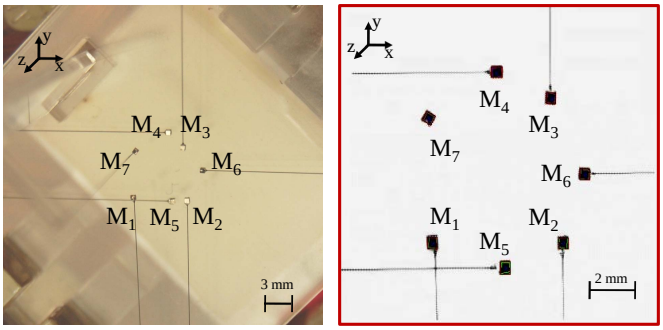

(a) (b)

Fig. 3: a) Prototype of the 8 DOF magnetic mechanism. b) Top view camera recording $x-y$ displacements. Video is available in supplementary materials.

TABLE IV: Test inputs to calibrate the 8 DOF magnetic mechanism.

	$\frac{\partial B_x}{\partial x}$ (T/m)	$\frac{\partial B_x}{\partial y}$ (T/m)	$\frac{\partial B_x}{\partial z}$ (T/m)	$\frac{\partial B_y}{\partial y}$ (T/m)	$\frac{\partial B_y}{\partial z}$ (T/m)	B_x(mT)	B_y(mT)	B_z(mT)
Input 1	0.5	0.0	0.0	0.0	0.0	0.0	0.0	0.0
Input 2	0.0	0.5	0.0	0.0	0.0	0.0	0.0	0.0
Input 3	0.0	0.0	0.5	0.0	0.0	0.0	0.0	0.0
Input 4	0.0	0.0	0.0	0.5	0.0	0.0	0.0	0.0
Input 5	0.0	0.0	0.0	0.0	0.5	0.0	0.0	0.0
Input 6	0.0	0.0	0.0	0.0	0.0	5.0	0.0	0.0
Input 7	0.0	0.0	0.0	0.0	0.0	0.0	5.0	0.0
Input 8	0.0	0.0	0.0	0.0	0.0	0.0	0.0	5.0

TABLE V: Calibration results for the 8 DOF magnetic mechanism.

	$d_1(\mu$m)	$d_2(\mu$m)	$d_3(\mu$m)	$d_4(\mu$m)	$d_5(\mu$m)	$d_6(\mu$m)	$d_7(\mu$m)	$d_8(\mu$m)
Input 1	900	240	-80	-20	-260	0	680	60
Input 2	360	640	-80	-580	60	20	120	-640
Input 3	-80	220	620	120	220	0	-80	-20
Input 4	120	60	-40	-260	-720	-60	-160	-100
Input 5	-140	-80	80	0	40	-620	-40	-60
Input 6	-20	540	-20	20	420	20	20	-20
Input 7	-560	20	0	-340	-40	20	20	0
Input 8	0	20	20	-20	0	40	520	-60

To verify the capability of the system in individually actuating each DOF, eight open-loop experiments were conducted; duration of each 5 seconds and designed to displace d_i from 0 to 600 μm (linear ramp profile). As plotted data in Fig. 4 shows, during each experiment, the targeted output followed the desired trajectory and the rest of seven outputs remained close to zero. In order to investigate system performance in terms of independent actuation of DOFs, we defined cross-talk for each DOF, as maximum deflection occurred during experiments which ideally should not affect d_i, divided by its maximum deflection during its designated experiment. Cross-talk for each one of DOFs are reported in Table VI, where the maximum belongs to d_1 which is 8.6%.

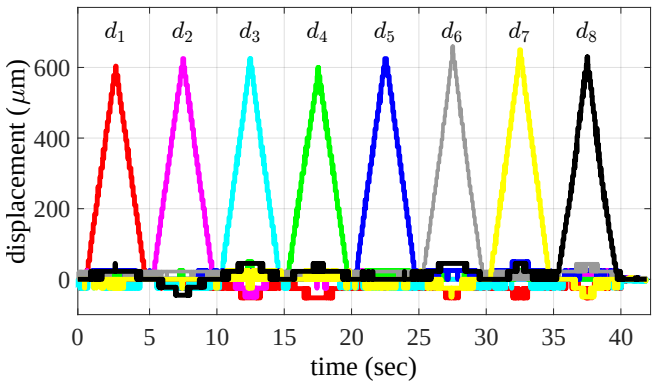

Fig. 4: Validating 8 DOF magnetic mechanism through eight sets of open-loop experiments; duration of each is 5 s, and is designed to displace d_i from 0 to 600 μm (linear ramp profile). Video is available in supplementary materials.

TABLE VI: 8 DOF Magnetic System cross-talk; calculated for each DOF as maximum non-diagonal element divided by corresponding diagonal element.

	$d_1(\mu m)$	$d_2(\mu m)$	$d_3(\mu m)$	$d_4(\mu m)$	$d_5(\mu m)$	$d_6(\mu m)$	$d_7(\mu m)$	$d_8(\mu m)$
0-5 (s)	**603**	0	-25	25	25	22	0	22
5-10 (s)	-26	**625**	-25	0	0	22	0	-45
10-15 (s)	-52	-50	**625**	50	25	22	0	45
15-20 (s)	-52	0	0	**600**	0	22	25	45
20-25 (s)	-26	0	-25	0	**625**	22	-25	0
25-30 (s)	-52	0	0	25	25	**660**	-25	45
30-35 (s)	-52	25	0	25	50	0	**650**	45
35-40 (s)	-26	0	0	0	25	44	-50	**630**
Cross-Talk	8.6%	8%	4%	8.3%	8%	6.6%	7.7%	7.1%

V. CONCLUSIONS

This paper studies, for the first time, how to utilize maximum number of magnetic field parameters at a single point in the workspace to allow for maximum possible DOFs, which is eight. In this work, we have developed an 8 DOF millimeter-scale magnetic mechanism as a proof of concept to demonstrate maximum capabilities of uniform steady magnetic fields in independently controlling remote magnetic agents. These results serve as a general framework which will potentially allow for developing future magnetic systems with maximum dexterity, specifically in applications such as multi-agent or flexible mechanisms where more DOFs are needed to be controlled. Our future work will be focused on developing a generalized framework to apply this theory on any mechanism with desired constraints and DOFs, and we will use this framework to design functional microrobotic devices.

REFERENCES

[1] T. Honda, K. Arai, and K. Ishiyama, "Micro swimming mechanisms propelled by external magnetic fields," *IEEE Transactions on Magnetics*, vol. 32, no. 5, pp. 5085–5087, 1996.

[2] M. P. Kummer, J. J. Abbott, B. E. Kratochvil, R. Borer, A. Sengul, and B. J. Nelson, "Octomag: An electromagnetic system for 5-dof wireless micromanipulation," *IEEE Transactions on Robotics*, vol. 26, no. 6, pp. 1006–1017, 2010.

[3] B. R. Donald, C. G. Levey, and I. Paprotny, "Planar microassembly by parallel actuation of mems microrobots," *Journal of Microelectromechanical Systems*, vol. 17, no. 4, pp. 789–808, 2008.

[4] A. A. Solovev, Y. Mei, E. Bermúdez Ureña, G. Huang, and O. G. Schmidt, "Catalytic microtubular jet engines self-propelled by accumulated gas bubbles," *Small*, vol. 5, no. 14, pp. 1688–1692, 2009.

[5] O. Sul, M. Falvo, R. Taylor, S. Washburn, and R. Superfine, "Thermally actuated untethered impact-driven locomotive microdevices," *Applied Physics Letters*, vol. 89, no. 20, p. 203512, 2006.

[6] H. Maruyama, T. Fukuda, and F. Arai, "Laser manipulation and optical adhesion control of functional gel-microtool for on-chip cell manipulation," in *Intelligent Robots and Systems, 2009. IROS 2009. IEEE/RSJ International Conference on*. IEEE, 2009, pp. 1413–1418.

[7] B. Behkam and M. Sitti, "Bacterial flagella-based propulsion and on/off motion control of microscale objects," *Applied Physics Letters*, vol. 90, no. 2, p. 023902, 2007.

[8] E. B. Steager, M. S. Sakar, C. Magee, M. Kennedy, A. Cowley, and V. Kumar, "Automated biomanipulation of single cells using magnetic microrobots," *The International Journal of Robotics Research*, vol. 32, no. 3, pp. 346–359, 2013.

[9] C. Pawashe, S. Floyd, and M. Sitti, "Modeling and experimental characterization of an untethered magnetic micro-robot," *The International Journal of Robotics Research*, vol. 28, no. 8, pp. 1077–1094, 2009.

[10] P. Berkelman and M. Dzadovsky, "Magnetic levitation over large translation and rotation ranges in all directions," *IEEE/ASME Transactions on Mechatronics*, vol. 18, no. 1, pp. 44–52, 2013.

[11] D. Wong, E. B. Steager, and V. Kumar, "Independent control of identical magnetic robots in a plane," *IEEE Robotics and Automation Letters*, vol. 1, no. 1, pp. 554–561, 2016.

[12] A. Becker, O. Felfoul, and P. E. Dupont, "Simultaneously powering and controlling many actuators with a clinical mri scanner," in *2014 IEEE/RSJ International Conference on Intelligent Robots and Systems*. IEEE, 2014, pp. 2017–2023.

[13] A. Ghosh and P. Fischer, "Controlled propulsion of artificial magnetic nanostructured propellers," *Nano letters*, vol. 9, no. 6, pp. 2243–2245, 2009.

[14] J. Zhang, P. Jain, and E. Diller, "Independent control of two millimeter-scale soft-bodied magnetic robotic swimmers," in *Robotics and Automation (ICRA), 2016 IEEE International Conference on*. IEEE, 2016, pp. 1933–1938.

[15] J. Zhang and E. Diller, "Millimeter-scale magnetic swimmers using elastomeric undulations," in *Intelligent Robots and Systems (IROS), 2015 IEEE/RSJ International Conference on*. IEEE, 2015, pp. 1706–1711.

[16] P. Ryan and E. Diller, "Five-degree-of-freedom magnetic control of micro-robots using rotating permanent magnets," in *Robotics and Automation (ICRA), 2016 IEEE International Conference on*. IEEE, 2016, pp. 1731–1736.

[17] E. Diller, J. Giltinan, and M. Sitti, "Independent control of multiple magnetic microrobots in three dimensions," *The International Journal of Robotics Research*, vol. 32, no. 5, pp. 614–631, 2013.

[18] E. Diller, J. Giltinan, G. Z. Lum, Z. Ye, and M. Sitti, "Six-degrees-of-freedom remote actuation of magnetic microrobots," in *Robotics science and systems*, 2014.

[19] A. J. Petruska and B. J. Nelson, "Minimum bounds on the number of electromagnets required for remote magnetic manipulation," *IEEE Transactions on Robotics*, vol. 31, no. 3, pp. 714–722, 2015.

[20] J. Zhang, O. Onaizah, K. Middleton, L. You, and E. Diller, "Reliable grasping of three-dimensional untethered mobile magnetic microgripper for autonomous pick-and-place," *IEEE Robotics and Automation Letters*, vol. 2, no. 2, pp. 835–840, 2017.